Chemistry and structure of BaTiO3 ultra-thin films grown by different O2 plasma power

J.L. Wang, J. Leroy, G. Niu, G. Saint-Girons, B. Gautier, B. Vilquin, N. Barrett

Chemical Physics Letters 592 (2014) 206–210

Contents lists available at ScienceDirect

Chemical Physics Letters

journal homepage: www.elsevier.com/locate/cplett

Chemistry and structure of $BaTiO_3$ ultra-thin films grown by different O_2 plasma power

J.L. Wang [a,*], J. Leroy [a], G. Niu [b], G. Saint-Girons [b], B. Gautier [c], B. Vilquin [b], N. Barrett [a]

[a] CEA, IRAMIS, SPCSI, LENSIS, F-91191 Gif sur Yvette cedex, France
[b] Université de Lyon, Ecole Centrale de Lyon, Institut des Nanotechnologies de Lyon, F-69134 Ecully cedex, France
[c] Université de Lyon, INSA Lyon, Institut des Nanotechnologies de Lyon, F-69621 Villeurbanne cedex, France

ARTICLE INFO

Article history:
Received 31 August 2013
In final form 14 December 2013
Available online 19 December 2013

ABSTRACT

We present a study of the chemical and atomic properties of 5 nm TiO_2-terminated $BaTiO_3$ (001) epitaxial films on Nb-doped $SrTiO_3$, as a function of the atomic oxygen plasma power for film growth. Lower plasma power produces non-stoichiometric films with oxygen vacancies and Ti^{3+} ions. The larger Ti^{3+} ion radius and the in-plane clamping gives rise to an increase in the out-of-plane lattice parameter. XPS measures the Ti^{3+} concentration and the concomitant increase in dissociative water uptake in the film, giving rise to on-top OH^- adsorption on surface Ti, proton adsorption on surface oxygen, and a near surface Ba-OH environment.

1. Introduction

Ferroelectric (FE) materials have attracted much attention, not only because of their fascinating electronic properties, but also their promising applications in electronic devices such as nonvolatile FE memories. They are therefore of both fundamental scientific interest and great practical importance [1,2]. One of the most important issues in ferroelectric perovskite oxide, of general chemical formula ABO_3, is the role of oxygen vacancies, Vo, which are omnipresent after crystal or thin film growth [3]. The oxygen atmosphere during growth can strongly influence the Vo concentration. Oxygen vacancies can be charged, trapping one or two electrons, or neutral, donating two electrons per vacancy which can reduce the B-type cation, for example Ti^{4+} to Ti^{3+} in $BaTiO_3$ (BTO). Thus, Vo can significantly influence the conductivity and the optical absorption properties of the oxide film [3,4]. In addition, Vo plays a role surface chemistry, for example by enhancing adsorption and dissociation of simple molecules such as H_2O [5,6]. These phenomena have been discussed in terms of the loss of performance in ferroelectric capacitors [7–10], and of the screening of polarized ferroelectric surfaces [11]. High quality, single crystal, epitaxial films of perovskite oxides can be produced using molecular beam epitaxy (MBE) [12]. Atomic oxygen, thanks to its higher reactivity, can make a large difference in the oxidation state of the cations as compared to molecular oxygen. For BTO the use of atomic oxygen promotes the oxidation of metals and improve the dielectric properties of oxide thin films, thus improves the ferroelectric properties [13].

In this Letter, we report an experimental study of chemical and atomic structural properties of strained TiO_2-terminated BTO (001) epitaxial films on a Nb-doped $SrTiO_3$(STO) substrate as a function of atomic oxygen plasma power. The structure and epitaxial strain of BTO is measured using X-ray diffraction (XRD) and the film chemistry and stoichiometry is studied using X-ray photoelectron spectroscopy (XPS).

2. Experiment details

The commercial STO (001) substrate with an optical mirror surface finish was etched with buffered NH_4F–HF solution (BHF) and then annealed in O_2 to obtain a TiO_2-terminated surface composed of steps and atomically flat terraces following the established protocol [6]. After heating the substrate to 650 °C for 1 h under an oxygen partial pressure of $\sim 10^{-6}$ Torr to remove carbon contamination on the surface, 5-nm-thick TiO_2-terminated BTO films were grown on this substrate by MBE with a growth rate of ~1 ML/min. The thickness of a fully strained BTO monolayer on STO is around 0.42 nm, thus around 12 BTO MLs were grown. The metallic Ba and Ti were put in the Knudsen cells heated by resistance coil to produce the vapor flux. During growth, the atomic oxygen partial pressure was kept at 5×10^{-6} Torr and the substrates maintained at 630 °C to get an atomically flat surface. The atomic oxygen is produced with an ADDON plasma cell. The growth of the BTO was monitored by in situ RHEED which allowed a precise control of the number of atomic layers. At 5 nm the Ba source was switched off ensuring deposition of a TiO_2 last layer. Films were grown with atomic oxygen plasma powers of 250, 400 and 550 W.

* Corresponding author. Fax: +33 (0)1 69 08 84 46.
E-mail address: jialewang@live.com (J.L. Wang).

0009-2614/$ - see front matter © 2013 Elsevier B.V. All rights reserved.
http://dx.doi.org/10.1016/j.cplett.2013.12.030

The crystal structure of the samples was measured by high-resolution X-ray diffraction (six-circles Rigaku SmartLab diffractometer with rotative anode using Cu $K\alpha_1$ line, $\lambda = 1.5406$ Å) in the θ–2θ mode for out-of-plane scans and φ–2θ for in-plane scans.

XPS was carried out using a hemispherical analyzer with a 128-channel strip anode detector and a monochromatic Al Kα (1486.7 eV) X-ray source (both from Omicron Nanotechnology GmbH) in a third chamber. Before insertion into the UHV system the samples were ozone cleaned for 10 min to remove carbon contamination on the surface. The analyzer pass energy of 40 eV gave an overall energy resolution (photons and spectrometer) of 0.5 eV. The binding energy scale was calibrated using the C 1s line at 284.6 eV as a reference. Take-off angles of 90° (normal emission) and 30° (grazing emission) were used to distinguish between surface and sub-surface chemistry. The data were analyzed using the CasaXPS software which employs a linear least squares optimization with a peak fitting algorithm. Shirley backgrounds were subtracted from the data as part of the curve fitting process.

3. Results

Figure 1 shows the XRD scans of the three BTO films grown using 250, 400 and 550 W plasma powers. For the in-plane scans of Figure 1a, the main peak located at $2\theta = 32.38°$ corresponds to the STO (1 1 0) reflection from the substrate [14]. The structure at the low 2θ angle (32°) with respect to the STO peak position corresponds to the (1 1 0) peak of in-plane compressively strained BTO film and does not change with plasma power. Figure 1b presents the out-of-plane XRD scans. The main peak at $2\theta = 46.48°$ is the STO (0 0 2) reflexion. The shoulder at lower 2θ with respect to the STO peak is the (0 0 2) peak of the BTO. It shifts to larger angles for higher oxygen plasma power. The c-axis values are 4.160, 4.153 and 4.148 Å for 250, 400 and 500 W, respectively. Thus, as the plasma power increases the out-of-plane lattice parameter decreases whereas the in-plane lattice constant, clamped by the epitaxial growth on the substrate, remains constant. The broadening of out-of-plane signal of BTO is because of the small thickness of BTO film. Due to Scherrer equation, the FWHM is around 2.2° corresponding to a 5-nm-thick BTO film. However, the low thickness results in a poor signal-background ratio.

The C 1s peak in the XPS survey scans of Figure 2 shows that there is only a small amount of surface C contamination, suggesting that the surface is clean with very low carbon contamination. The Ba $3d_{5/2}$, Ti $2p_{3/2}$ and O 1s XPS core level spectra are shown in Figures 3–5 at normal and grazing emission.

The Ba $3d_{5/2}$ spectra of samples grown using 250, 400 and 550 W oxygen plasma power are shown in Figure 3a–c. The main peak, labeled I, has a binding energy (BE) of 778.5 eV and is due

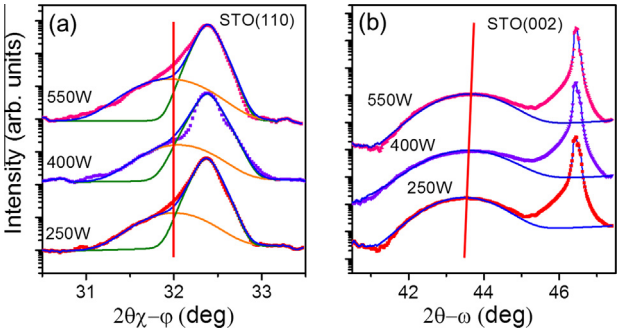

Figure 1. (a) In-plane and (b) out-of-plane scan XRD spectra of samples grown with 250, 400 and 550 W O_2 plasma power. The two peaks located at $2\theta = 32.38°$ (in-plane scan) and 46.48° (out-of-plane scan) are due to STO (1 1 0) and STO (0 0 2) reflections, respectively.

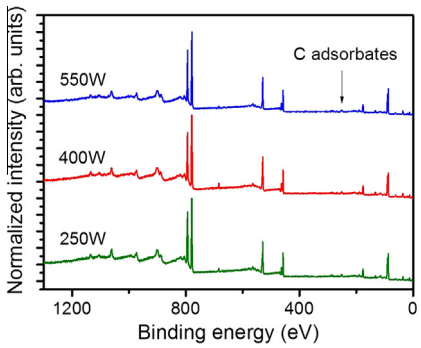

Figure 2. XPS survey spectra of 5 nm BTO films grown using 250, 400 and 550 W plasma power. Note the very low C 1s level indicating an almost C-free surface.

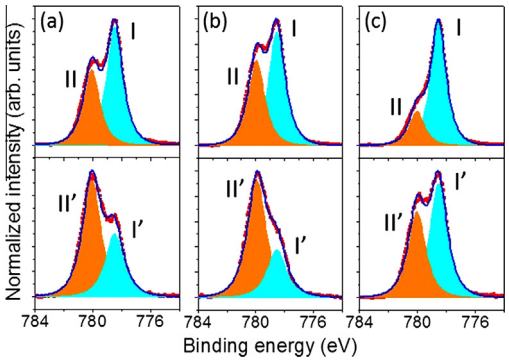

Figure 3. Ba $3d_{5/2}$ XPS core level spectra on BTO thin films grown with: (a) 250 W; (b) 400 W; (c) 550 W O_2 plasma power at normal (top) and 30° (bottom) take-off angle angles.

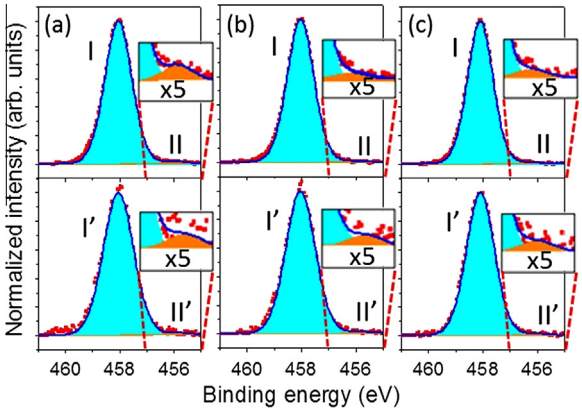

Figure 4. Ti $2p_{3/2}$ XPS core level spectra on BTO thin films grown with: (a) 250 W; (b) 400 W; (c) 550 W O_2 plasma power at normal (top) and 30° (bottom) take-off angle angles. The insets show the Ti_{II} peaks amplified by 5 times.

to bulk-coordinated Ba. Each spectrum also has a component labeled II, shifted by 1.7 eV to high binding energy (HBE). The grazing emission angle spectra confirm that this HBE component is of surface origin. The peak has been interpreted as being due to the presence of surface species such as $Ba(OH)_2$ or $BaCO_3$ [15]. However, the absence of a C 1s peak shows that there is no significant surface carbonate species, therefore the HBE component cannot be due to $BaCO_3$ species. Furthermore, the films are TiO_2-terminated so we do not expect Ba in the top surface layer. The relative intensity of peak II is larger than that of 'dry' surface with very little residual

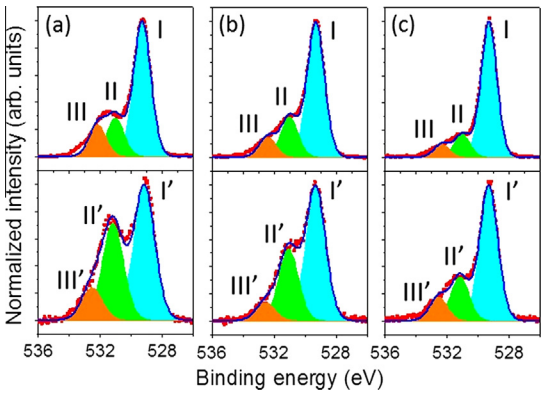

Figure 5. O 1s XPS core level spectra on BTO thin films grown with: (a) 250 W; (b) 400 W; (c) 550 W O_2 plasma power at normal (top) and 30° (bottom) take-off angle angles.

water [6]. Thus it may be due to the formation of Ba-OH bonds in the near surface region.

The Ti $2p_{3/2}$ spectra are presented in Figure 4. The spectra have a main component (BE = 458 eV) due to Ti with a formal valency of 4+ as in the perovskite structure, and a very weak component, shifted by 1.6 eV to low binding energy (LBE), corresponding to Ti^{3+}. This component is stronger at lower plasma power.

Figure 5 shows the O 1s spectra. The spectrum has three components, peak I with a BE of 529.4 eV is due to oxygen in the perovskite environment [15]. Peak II (BE = 531.0 eV) is clearly has a surface origin, as can be seen by comparison between 90° and 30° take-off angle spectra. O_{II} has been attributed to oxygen in lattice positions coordinated with a proton [6] whereas O_{III} (BE = 532.2 eV) is ascribed to hydroxyl groups chemically bonding to surface and near surface Ti and Ba cations observed even in 'dry' samples [5]. It may therefore partly be the oxygen counterpart to the Ba_{II} peak. The O_{II} intensity increases for lower plasma power whereas the O_{III} intensity is constant.

The Sr 3d spectra from the STO substrate are presented in Figure 6a–c showing the spin–orbit split $3d_{5/2}$ and $3d_{3/2}$ emission. The binding energy is constant indicating that the substrate chemistry is not affected by the plasma power. The Sr 3d intensity has been used to estimate the thickness of the films to be 5 nm, respectively. The mean-free path has been calculated using the National Institute of Standards and Technology (NIST) database [16], and as a first approximation we have that the films have the bulk mass density of BTO.

4. Discussion

4.1. Film chemistry

During the MBE growth, the oxygen plasma produces more reactive, atomic oxygen allowing control of the oxygen stoichiometry. The plasma power can therefore be used to adjust the Vo concentration and hence the lattice constant as already reported in ABO_3 perovskite oxides [17–20]. The stoichiometric deviation is accommodated by a reduction in the cation valency, normally the Ti ion next to the Vo. In ABO_3 oxides, reduction of the B-type cation from nominal high-valence state to a lower valence state gives rise to a higher lattice parameter as a result of expansion of the BO_6 octahedron volume by the distorted Jahn–Teller effect [18]. In BTO, two Ti^{4+} ions can be reduced to Ti^{3+} ions for each Vo. The chemical formula of the BTO thin films may therefore be written as [19]:

$$Ba^{2+}Ti^{4+}_{1-2x}Ti^{3+}_{2x}O^{2-}_{3-x}$$

where x is the Vo concentration with respect to the stoichiometric compound. The effective ionic radii for Ti^{4+} and Ti^{3+} are 0.605 and 0.670 Å, respectively [21]. Thus, the change of the Ti ion valency not only accommodates the Vo but also leads to an increase of the ionic radius of Ti and thus to an expansion of the unit cell volume. Due to in-plane clamping by the STO substrate as observed in the in-plane XRD scan, volume expansion can only occur perpendicular to the film and thus leads to a larger c-axis lattice parameter. In other words, the lower the plasma power, the higher the Vo concentration and, as a consequence, the larger the *c*-axis lattice constant. The co-existence of a- and c-type domains has been reported [22]. However, even in this case the same qualitative conclusion that the lower the plasma power, the higher the Vo concentration and thus larger *c*-axis lattice constant would apply.

The relative intensities of the Ba $3d_{5/2}$, Ti $2p_{3/2}$ and O 1s core level components are reported in Table 1. The bulk and surface components of Ti^{3+} decrease from 1.5% and 1.7% (250 W) to 1.3% and 1.4% (400 W), then finally 0.9% and 1.2% (550 W), confirming that the Vo concentration decreases as the plasma power increases. From the Ti^{3+} intensity, the remaining surface Vo concentration can be estimated to be around 0.3% with respect to the total number of oxygens. The value is even lower than that of a dry surface [6], which suggests that there may be some recovery mechanism of the Vo.

The inelastic mean free path of the Sr 3d electrons is 1.81 nm [16]. Thus, the Sr-3d spectra are particularly sensitive to the chemical environment at the BTO/STO interface for 5 nm films. The Sr 3d spectra show no HBE component, often observed on clean STO surfaces [15,23] or at the interface of a non-epitaxial interface [14]. In our case, because of the high quality epitaxy of the BTO there is no free STO surface, and the Sr at the interface has a bulk-like, perovskite coordination. The absence of an observable core level shift is strong evidence for a sharp interface without interdiffusion.

The film stoichiometry as calculated from Ba 3d, Ti 2p and O 1s core level intensities and the Scofield atomic cross-sections [24] at normal and grazing emission is given in Table 2. The proportion of oxygen increases with plasma power which is consistent with lower Vo concentration although the differences are close to the XPS sensitivity limit. The samples grown with 250 and 400 W plasma are Ba-rich but Ti depleted. At 550 W there is slight O-enrichment.

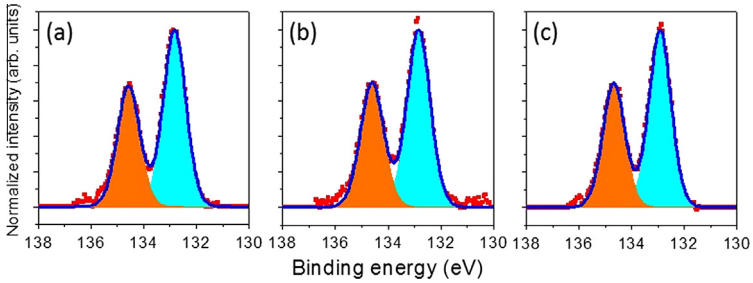

Figure 6. Sr 3d spectra from the STO substrate under the films: (a) 250 W; (b) 400 W; (c) 550 W O_2 plasma power at normal emission.

Table 1
Relative intensities of the Ba 3d, Ti 2p and O 1s core level components at normal and 30° emission.

	250 W		400 W		550 W	
	Bulk sensitive	Surface sensitive	Bulk sensitive	Surface sensitive	Bulk sensitive	Surface sensitive
BaI	57.3	29.0	61.1	35.0	78.3	57.1
BaII	42.7	71.0	38.9	65.0	21.7	42.9
Ti4+	98.5	98.3	98.7	98.6	99.1	98.8
Ti3+	1.5	1.7	1.3	1.4	0.9	1.2
OI	65.8	50.9	68.9	59.7	78.9	66.7
OII	18.8	36.8	20.6	32.1	13.4	21.6
OIII	15.4	12.3	10.5	8.2	7.7	11.7

Table 2
Stoichiometric proportion between Ba, Ti and O calculated from Ba 3d, Ti 2p and O 1s core level components at normal and 30° emission.

	250 W		400 W		550 W	
	Bulk sensitive	Surface sensitive	Bulk sensitive	Surface sensitive	Bulk sensitive	Surface sensitive
Ba	0.21	0.22	0.20	0.21	0.19	0.17
Ti	0.17	0.17	0.18	0.19	0.18	0.19
O	0.62	0.61	0.62	0.60	0.63	0.64

4.2. Water uptake

One direct consequence of the non-stoichiometry appears to be the water uptake by the film. This is an important point since H^+ and OH^- species can drastically affect the ferroelectric polarization [25–27]. The XPS core level provides detailed information on the correlation between water uptake and oxygen vacancy concentration.

From the Ti^{3+} intensity, the surface Vo concentration is around 0.3% The O_{II} (O_{III}) intensities is 18.8 (15.4)%, 20.6 (10.5)% and 13.4 (7)% for plasma power of 250, 400 and 550 W, respectively. If only surface oxygen atoms were involved in adsorption then the core level intensity should give a simple quantitative measurement of the H_2O dissociation. We consider each layer as a homogeneous medium but take into account the layer by layer stoichiometry TiO_2–BaO–TiO_2–... Letting I^O denotes the O 1s intensities from an O atom, this leads to the following expressions for the total O 1s intensities:

$$I^{TOT}(O1s) = I^O(k+2)/(1-k^2)$$

where the layer attenuation factor is given by $k = \exp(-c/\lambda \cdot \sin\theta)$, λ is the inelastic mean free path and θ the take-off angle with respect to the sample surface. The λ for the O 1s emission is assumed to be 1.1 nm [16,17]. If the O_{II} peak were only from surface layer then the 30° take-off angle results would suggest that 46.0% of the surface oxygen atoms are coordinated with protons for the sample grown with 550 W plasma power. This estimation rises to 58.6% and 65.6% for 400 W and 250 W plasma powers. The normal emission intensities suggest 44.1%, 58.2% and 57.0% for 550, 400 and 250 W plasma powers. The O_{II} peak may also be due to uptake of hydrogen in UHV during growth in agreement with the observations of Kobayashi et al. [28], who point out the thermal diffusion of hydrides.

The surface sensitive O_{III} intensities, representing the OH^- coordinated cations, spectrum are 21.7%, 13.9% and 19% of the total O 1s intensity for plasma powers of 250, 400 and 550 W, respectively. The O_{III} corresponds to OH^- chemically bonded on top to surface Ti atoms. The evolution of the Ba $3d_{5/2}$ XPS spectra presented in Figure 3 indicates the increasing presence of near-surface Ba-OH species at lower plasma power. By using the same estimate of the photoelectron inelastic mean free path and the layer by layer attenuation as applied to the previous oxygen analysis, we would expect the surface related peaks proportions of the Ba 3d intensity change from 49.4% to 76.1% with plasma power decreasing from 550 to 400 W. Since oxygen vacancy is a water dissociative adsorption site, water bond to a surface near an oxygen vacancy can form an OH^- ion and a proton, H^+. The OH^- fills the oxygen vacancy site and the proton moves inside bulk, coordinating with a lattice oxygen to form another OH^-, thus Ba-OH [6]. The increase of the O_{II} component at lower plasma power is therefore consistent with the existence of more Vo sites. The increasing of Ba_{II} peak corresponds to the formation of more Ba-OH near the surface. The slight decrease in the Ba_{II} intensity to 70.7% of the total intensity for the film grown at 250 W may be correlated with the formation of hydroxyl group on top of surface Ti sites.

Dissociative adsorption of water at the BTO surface gives rise to protons which can bond to lattice oxygens (O_{II}) [6] and OH^- groups which either bond to cations (O_{III}) or fill oxygen vacancy sites (O_{II}) [15]. We can therefore estimate the number of Vo sites filled by OH^- as being represented by $\frac{1}{2}(O_{II} - O_{III})$ in the core level intensity and the lattice oxygens coordinated with protons as $\frac{1}{2}(O_{II} + O_{III})$. These values are also reported in Table 1. Vo sites favor dissociation [5] and are preferentially found at the surface. The increase of the O_{II} intensity in the O 1s XPS spectrum for lower plasma power is therefore consistent with higher initial Vo concentration on film growth. The O_{III} corresponds to OH^- on-top bonding at a surface Ti site but given the strength of the Ba_{II} peak we deduce that it may also represent OH^- coordinated Ba_I in the near surface region suggesting a high mobility of the OH^- ions after dissociation. The HBE component of the Ba 3d increases at lower plasma power, further supporting the interpretation that additional hydroxyl groups coming from enhanced dissociative adsorption due to the Vo sites contribute to Ba-OH near surface bonding.

5. Conclusion

XRD and XPS has been used to study the atomic, electronic and chemical properties on strained TiO_2-terminated BTO (001) epitaxial film on a $SrTiO_3$ substrate grown under atomic oxygen produced by a plasma cell with different plasma powers of 250, 400 and 550 W. X-ray diffraction shows that with a decrease of the oxygen plasma power, the *c*-axis lattice constant of the BTO films become larger, owing to an increase of the oxygen vacancies. XPS

results confirmed the existence of Ba-OH in the films because of water dissociative adsorption on oxygen vacancies sites and thus creating hydroxyl groups. The concentration of Ba-OH increases with lower plasma power used for sample growth.

Acknowledgements

This work was supported by the French National Research Agency (ANR) project Surf-FER, ANR-10-BLAN-1012.

References

[1] R. Ramesh, D.G. Schlom, Science 296 (2002) 1975.
[2] C.H. Ahn, K.M. Rabe, J.-M. Triscone, Science 303 (2004) 488.
[3] H. Donnerberg, A. Birkholz, J. Phys. Condens. Matter 12 (2000) 8239.
[4] D.M. Smyth, Prog. Solid State Chem. 15 (1984) 145.
[5] S. Wendt et al., Phys. Rev. Lett. 96 (2006) 066107.
[6] J.L. Wang et al., J. Phys. Chem. C 116 (2012) 21802.
[7] Y. Shimamoto, K. Kushida-Abdelghafar, H. Miki, Y. Fujisaki, Appl. Phys. Lett. 70 (1997) 3096.
[8] J.P. Han, T.P. Ma, Appl. Phys. Lett. 71 (1997) 1267.
[9] S. Zafar et al., J. Appl. Phys. 82 (1997) 4469.
[10] J. Im et al., Appl. Phys. Lett. 74 (1999) 1162.
[11] J.L. Wang, B. Vilquin, N. Barrett, Appl. Phys. Lett. 89 (2006) 112904.
[12] D.G. Schlom, L.-Q. Chen, X.Q. Pan, A. Schmehl, M.A. Zurbuchen, J. Am. Ceram. Soc. 91 (2008) 2429.
[13] G. Niu et al., Thin Solid Films 520 (2012) 4595.
[14] J.L. Wang et al., Phys. Rev. B 84 (2011) 205426.
[15] J.D. Baniecki, M. Ishii, T. Shioga, K. Kurihara, S. Miyahara, Appl. Phys. Lett. 89 (2006) 162908.
[16] C.J. Powell, A. Jablonski (Eds.), NIST Electron Inelastic-Mean-Free-Path Database-Version 1.2, National Institute of Standards and Technology, Gaithersburg, 2010.
[17] Z.T. Xu et al., Small 8 (2012) 1279.
[18] L. Qiao, X.F. Bi, Thin Solid Films 529 (2010) 943.
[19] H.L. Cai, X.S. Wu, J. Gao, Chem. Phys. Lett. 467 (2009) 313.
[20] S.B. Mi, C.L. Jia, T. Heeg, O. Trithaveesak, J. Schubert, K. Urban, J. Cryst. Growth 283 (2005) 425.
[21] R. Perez-Casero et al., Phys. Rev. B 75 (2007) 165317.
[22] G. Sheng et al., Appl. Phys. Lett. 93 (2008) 232904.
[23] G.M. Vanacore, L.F. Zagonel, N. Barrett, Surf. Sci. 604 (2010) 1674.
[24] J.H. Scofield, Theoretical Photoionization Cross Sections from 1 to 1500 keV, Lawrence Livermore National Laboratory, Report UCRL-51 326, 1973.
[25] J. Shin et al., Nano. Lett. 9 (2009) 3720.
[26] G. Geneste, B. Dkhil, Phys. Rev. B 79 (2009) 235420.
[27] C.H. Park, D.J. Chadi, Phys. Rev. Lett. 84 (2000) 4717.
[28] Y. Kobayashi et al., Nat. Mater. 11 (2012) 507.